

## **A Curvilinear Frame Element with Plastic Hinges**

**Julio Flórez-López**

Structural Engineering Department  
University of Los Andes, Venezuela  
Structural Engineering Department  
São Carlos School of Engineering, University of São Paulo, Brazil  
[iflorez@ula.ve](mailto:iflorez@ula.ve)

**Sergio P. B. Proença**

Structural Engineering Department  
São Carlos School of Engineering, University of São Paulo, Brazil  
[persival@sc.usp.br](mailto:persival@sc.usp.br)

...

### **ABSTRACT**

The concept of frame cannot be considered simply as the result of the application of the finite element procedure to the Euler-Bernoulli theory of beams. The difference between both approaches lies in the inclusion of the notion of plastic hinge in the theory of frames. A plastic hinge is not the consequence of the introduction of some approximate displacement field in the kinematic equations but a radical modification of the constitutive laws. As a result, a beam finite element and a frame element are not only quantitatively dissimilar but, most important, qualitatively different. This is especially significant in the case of structures presenting softening with all the associated localization problems. There is a large number of frame elements available in the literature but, as far as the authors know, all of them correspond to straight components. In the present work, a curvilinear frame element for arches with plastic hinges exhibiting hardening and/or softening is proposed and numerically validated.

**Keywords:** Circular arches, Finite element, Theory of Plasticity, Plastic Hinges

### **1 INTRODUCTION**

One of the most valuable advantages of the frame theory with plastic hinges is that the analyst has control over the way and the position where inelastic effects may be located in the structure. Often, this is a fundamental feature for an adequate and effective description of the structural behavior in the presence of softening.

A large number of frame elements with plastic hinges, which include not only plasticity but cracking or local buckling too, can be found in the literature. However, as far as the authors of this paper know, all of them correspond to straight components. On the other hand, arches are important structural alternatives in the construction industry. Many civil and aerospace structures may be modeled as arches. At the present time, an analyst using commercial finite element programs has to use beam elements or discretize the structure using many frame elements, which complicates unnecessarily the modeling of the structure and limits the control that the engineer has over the analysis. Circular and parabolic arch elements are available in the literature but they do not include

plastic hinges [1,2]. Notice that if lateral or in plane instability is controlled by providing sufficient bracing, the failure mechanism of the arch would be plastic collapse.

In this paper, a new frame element for circular arches with plastic hinges is proposed. The formulation accepts arbitrary yield functions and plastic evolution laws including hardening and/or softening. It is expected that in many practical applications, some users will find more convenient using a few circular frame elements instead of dense meshes of shell or beam elements. It is worth noting that analytical solutions for practical problems may be obtained, with the formulation presented in the paper, using any symbolic manipulator program.

The element was formulated from the classical theory of plasticity, using the notation introduced in [3] and the procedures described in [1,2].

## 2 STATICS AND KINEMATICS OF CIRCULAR ARCS

### 2.1 Kinematic equation

Consider a circular arch as shown in Fig. 1. A circular element between nodes  $i$  and  $j$  is isolated from the structure. The element is characterized by the radius  $R$  and the angle  $\alpha$ . Two sets of coordinates axes are defined: the global ( $X_G, Z_G$ ) and the local ones ( $x_L, z_L$ ). The angle between the axes  $Z_G$  and  $z_L$  is called  $\beta$ .

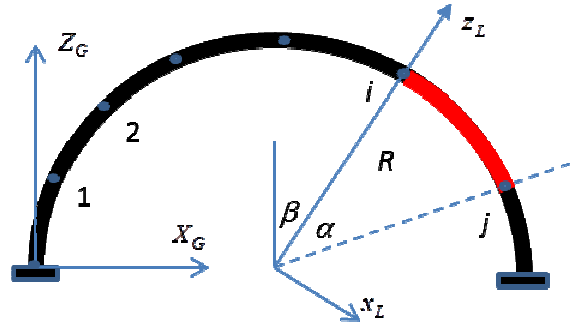


Figure 1 Circular arch, global and local coordinates axes

The angles  $\alpha$  and  $\beta$  can be computed as a function of the global coordinates of the element nodes and the element radius.

Two sets of static variables are introduced: the matrix of nodal forces in global coordinates:  $\{\mathbf{Q}\}^t = (Q_{ui}, Q_{wi}, Q_{\alpha}, Q_{uj}, Q_{wj}, Q_{\theta})$  (Fig 2a) and the matrix of generalized stresses in local coordinates:  $\{\mathbf{M}\}^t = (m_i, m_j, n_i)$  (Fig 2b). The variable  $m_i$  is the bending moment on the end  $i$  of the element,  $m_j$  is the bending moment on  $j$  and  $n_i$  is the axial force on  $i$  (compression is positive). Nodal forces matrices and generalized stresses are related by the following equilibrium equation:

$$\{\mathbf{Q}\} = [\mathbf{B}]^t \{\mathbf{M}\} \quad (1)$$

Where  $[\mathbf{B}]$  is denoted kinematic transformation matrix. The next section presents the explicit expression of this matrix.

Introduce now the matrices of nodal displacements  $\{\mathbf{q}\}^t = (u_i, w_i, \theta_i, u_j, w_j, \theta_j)$  and generalized deformations  $\{\Phi\}^t = (\phi_i, \phi_j, \delta)$ , that are conjugated with the nodal forces and generalized stresses respectively, then the power  $\dot{W}$  is computed as:

$$\dot{W} = \{\dot{\mathbf{q}}\}^t \{\mathbf{Q}\} = \{\dot{\Phi}\}^t \{\mathbf{M}\}; \quad \text{i.e.} \quad \{\dot{\mathbf{q}}\}^t [\mathbf{B}]^t \{\mathbf{M}\} = \{\dot{\Phi}\}^t \{\mathbf{M}\} \quad (2)$$

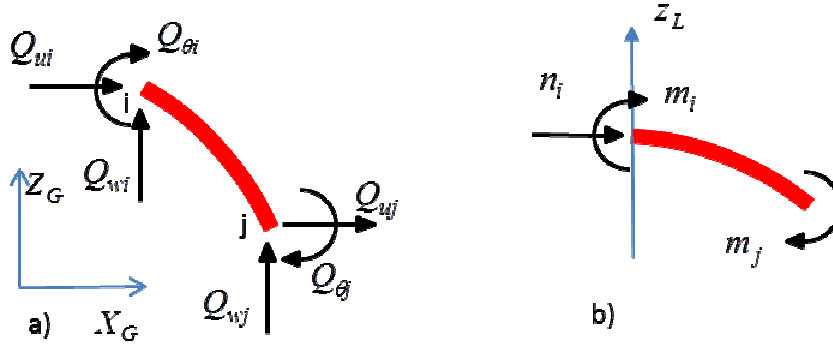


Figure 2 a) Nodal forces b) Generalized stresses

Therefore, these kinematic variables are related by the following equation:

$$\{\Phi\} = [\mathbf{B}] \{\mathbf{q}\} \quad (3)$$

The expression (3) is the kinematic equation of the curved element. If displacements are small, the transformation matrix in the initial and the deformed configurations ( $[\mathbf{B}_0]$  and  $[\mathbf{B}]$  respectively) are approximately the same, thus the kinematic and equilibrium equations become:

$$[\mathbf{B}] \cong [\mathbf{B}_0] \Rightarrow \{\Phi\} \cong [\mathbf{B}_0] \{\mathbf{q}\}; \quad \{\mathbf{P}\} \cong [\mathbf{B}_0]^t \{\mathbf{M}\} \quad (4)$$

## 2.2 Kinematic transformation matrix

Consider again the circular element in local coordinates and introduce a third static variable:  $\{\mathbf{Q}'\}^t = (Q'_{ui}, Q'_{wi}, Q'_{\theta i}, Q'_{uj}, Q'_{wj}, Q'_{\theta j})$ , the matrix of nodal forces again, but in local coordinates this time.

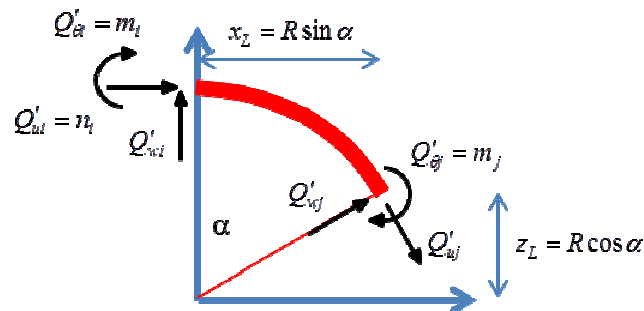


Figure 3 Nodal forces in local coordinates and generalized stresses

The equilibrium of the element is now defined by:

$$\begin{aligned}
 n_i + Q'_{uj} \cos \alpha + Q'_{wj} \sin \alpha &= 0 \\
 Q'_{wi} - Q'_{uj} \sin \alpha + Q'_{wj} \cos \alpha &= 0 \\
 m_i + n_i R(1 - \cos \alpha) + R Q'_{wi} \sin \alpha + m_j &= 0
 \end{aligned} \tag{5}$$

or in matrix equation:

$$\{Q'\} = [B']^t \{M\}; \quad [B'] = \begin{bmatrix} 0 & -\frac{1}{R \sin \alpha} & 1 & -\frac{1}{R} & \frac{\cos \alpha}{R \sin \alpha} & 0 \\ 0 & -\frac{1}{R \sin \alpha} & 0 & -\frac{1}{R} & \frac{\cos \alpha}{R \sin \alpha} & 1 \\ 1 & \frac{-1 + \cos \alpha}{\sin \alpha} & 0 & -1 & \frac{-1 + \cos \alpha}{\sin \alpha} & 0 \end{bmatrix} \tag{6}$$

Nodal forces in global coordinates  $\{Q\}$  and local coordinates  $\{Q'\}$  are related by the conventional geometrical transformation matrix  $[T]$ :

$$\{Q\} = [T] \{Q'\} \tag{7}$$

Where  $[T]$  is given by:

$$[T] = \begin{bmatrix} \cos \beta & \sin \beta & 0 & 0 & 0 & 0 \\ -\sin \beta & \cos \beta & 0 & 0 & 0 & 0 \\ 0 & 0 & 1 & 0 & 0 & 0 \\ 0 & 0 & 0 & \cos(\alpha + \beta) & \sin(\alpha + \beta) & 0 \\ 0 & 0 & 0 & -\sin(\alpha + \beta) & \cos(\alpha + \beta) & 0 \\ 0 & 0 & 0 & 0 & 0 & 1 \end{bmatrix} \tag{8}$$

Therefore:

$$[B] = [B'] [T]^t \tag{9}$$

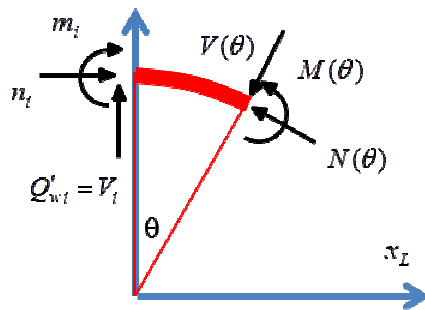


Figure 4. Bending moment, shear force and axial force in the arch

The bending moment, axial and shear forces (see Fig. 4) on any section of the element can also be expressed as a function of the generalized stresses by the same equilibrium considerations:

$$\begin{aligned}
 M(\theta) &= \frac{m_i \sin \alpha + n_i R \sin \alpha - n_i R \cos \theta \sin \alpha - m_i \sin \theta - n_i R \sin \theta + n_i R \sin \theta \cos \alpha - m_j \sin \theta}{\sin \alpha} \\
 V(\theta) &= \frac{-m_i \cos \theta - n_i R \cos \theta + n_i R \cos \theta \cos \alpha - m_j \cos \theta + n_i R \sin \alpha \sin \theta}{R \sin \alpha} \\
 N(\theta) &= \frac{m_i \sin \theta + n_i R \sin \theta - n_i R \sin \theta \cos \alpha + m_j \sin \theta + n_i R \sin \alpha \cos \theta}{R \sin \alpha}
 \end{aligned} \quad (10)$$

### 3 ELASTIC-PLASTIC CONSTITUTIVE EQUATIONS WITH PLASTIC HINGES

#### 3.1 Generalized plastic deformations in a circular element

Assume that the element is the assemblage of an elastic circular arch and two plastic hinges localized at its ends as shown in Fig 5.

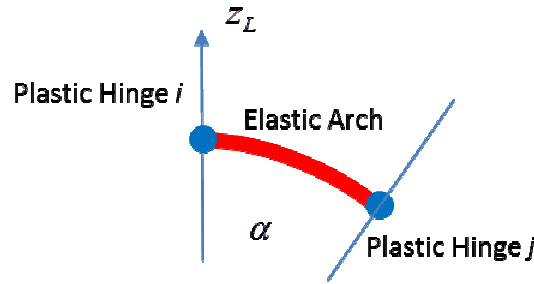


Figure 5. A circular arch element with two plastic hinges

These plastic hinges may experience rotations  $\theta_i^p$ ,  $\theta_j^p$  and/or elongations  $\Delta_i^p$ ,  $\Delta_j^p$  as shown in Fig. 6.

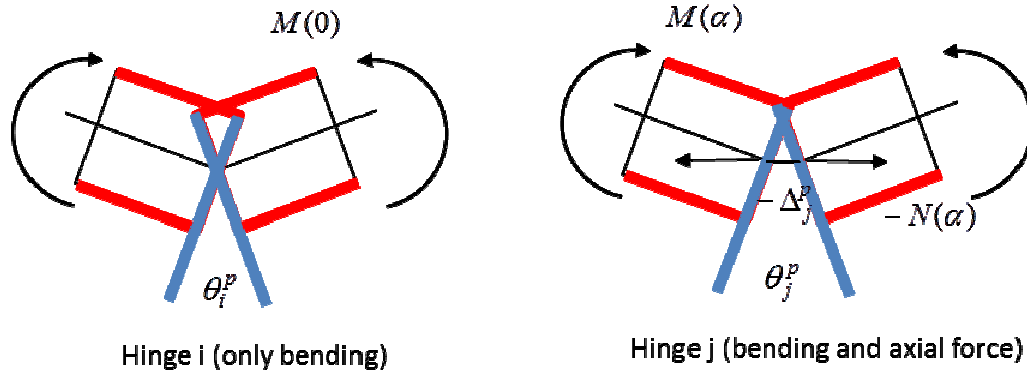


Figure 6. Plastic rotations and elongations a) without axial force b) with axial force

The plastic power  $\dot{W}_p$  of the plastic hinges is therefore:

$$\dot{W}_p = M(0)\dot{\theta}_i^p + N(0)\dot{\Delta}_i^p + M(\alpha)\dot{\theta}_j^p + N(\alpha)\dot{\Delta}_j^p \quad (11)$$

where  $M(0)$  is the bending moment of the plastic hinge  $i$ ,  $N(0)$  is the axial force on the same hinge and  $M(\alpha)$ ,  $N(\alpha)$  are the corresponding variables for hinge  $j$  (see Fig. 6).

On the other hand, assume that the total deformation matrix introduced in the previous section is expressed as the sum of an elastic part, the deformation of the elastic arch, and a plastic one:

$$\{\Phi\} = \{\Phi^e\} + \{\Phi^p\}; \quad \{\Phi^p\}^t = (\phi_i^p, \phi_j^p, \delta^p) \quad (12)$$

All the generalized deformation matrices in (12) are conjugated with the stress matrix  $\{\mathbf{M}\}$  giving, respectively, the total, elastic and plastic power on the element. Therefore, the latter is:

$$\dot{W}_p = m_i \dot{\phi}_i^p + m_j \dot{\phi}_j^p + n_i \dot{\delta}^p = M(0) \dot{\theta}_i^p + N(0) \dot{\Delta}_i^p + M(\alpha) \dot{\theta}_j^p + N(\alpha) \dot{\Delta}_j^p \quad (13)$$

According to (10):

$$M(0) = m_i; \quad N(0) = n_i; \quad M(\alpha) = -m_j; \quad N(\alpha) = \frac{m_i + n_i R + m_j}{R} \quad (14)$$

Thus, the equations (13-14) lead to:

$$\phi_i^p = \theta_i^p + \frac{\Delta_j^p}{R}; \quad \phi_j^p = -\theta_j^p + \frac{\Delta_j^p}{R}; \quad \delta^p = \Delta_i^p + \Delta_j^p \quad (15)$$

Expressions (15) give a physical interpretation of the internal variables  $(\phi_i^p, \phi_j^p, \delta^p)$ . Notice that  $\phi_i^p$  and  $\phi_j^p$  are not identical to the plastic rotations, but for large radii and small plastic elongations the difference is negligible. The term  $\delta^p$  is minus the total permanent elongation of the element.

### 3.2 Elasticity law

The elastic deformation term can be related to generalized stresses through the flexibility matrix  $[\mathbf{F}_0]$ :

$$\{\Phi^e\} = [\mathbf{F}_0] \{\mathbf{M}\} \quad (15)$$

Therefore, according to (12,15), the elasticity law of the circular element is:

$$\{\Phi - \Phi^p\} = [\mathbf{F}_0] \{\mathbf{M}\}; \quad \text{or}; \quad \{\mathbf{M}\} = [\mathbf{E}_0] \{\Phi - \Phi^p\} \quad (16)$$

where  $[\mathbf{E}_0] = [\mathbf{F}_0]^{-1}$  is the elasticity, or stiffness, matrix. The flexibility matrix terms can be obtained using the Castigliano theorem as described in [1,2]; the resulting expressions are given in the next section.

### 3.3 Flexibility matrix

The strain energy stored in a slender circular component can be written as:

$$U = \int_0^\alpha \left( \frac{M(\theta)^2}{2EI} + \frac{N(\theta)^2}{2AE} \right) R d\theta \quad (17)$$

where the terms  $EI$ , and  $AE$  are the usual bending and axial stiffness. Then, the coefficients of the flexibility matrix can be obtained according to Castigliano's theorem:

$$\begin{aligned} F_{11}^0 &= \frac{\partial^2 U}{\partial m_i \partial m_i} = \frac{1}{4} \frac{R(-8 \sin(\alpha) + 6\alpha - 4\alpha \cos(\alpha)^2 + 6 \sin(\alpha) \cos(\alpha))}{\sin(\alpha)^2 EI} - \frac{1}{4} \frac{-2\alpha + 2 \sin(\alpha) \cos(\alpha)}{R AE \sin(\alpha)^2} \\ F_{12}^0 &= \frac{\partial^2 U}{\partial m_i \partial m_j} = \frac{1}{4} \frac{R(-4 \sin(\alpha) + 2\alpha + 2 \sin(\alpha) \cos(\alpha))}{\sin(\alpha)^2 EI} - \frac{1}{4} \frac{-2\alpha + 2 \sin(\alpha) \cos(\alpha)}{R AE \sin(\alpha)^2} \\ F_{13}^0 &= \frac{\partial^2 U}{\partial m_i \partial n_i} = \frac{1}{4} \frac{R(-10 R \sin(\alpha) + 10 \sin(\alpha) R \cos(\alpha) - 2 R \cos(\alpha) \alpha + 6 R \alpha - 4 R \alpha \cos(\alpha)^2)}{\sin(\alpha)^2 EI} \\ &\quad - \frac{1}{4} \frac{-2 R \sin(\alpha) - 2 R \alpha + 2 \sin(\alpha) R \cos(\alpha) + 2 R \cos(\alpha) \alpha}{R AE \sin(\alpha)^2} \\ F_{22}^0 &= \frac{\partial^2 U}{\partial m_j \partial m_j} = \frac{1}{4} \frac{R(2\alpha - 2 \sin(\alpha) \cos(\alpha))}{\sin(\alpha)^2 EI} - \frac{1}{4} \frac{-2\alpha + 2 \sin(\alpha) \cos(\alpha)}{R AE \sin(\alpha)^2} \\ F_{23}^0 &= \frac{\partial^2 U}{\partial m_j \partial n_i} = \frac{1}{4} \frac{R(-2 R \sin(\alpha) - 2 R \cos(\alpha) \alpha + 2 R \alpha + 2 \sin(\alpha) R \cos(\alpha))}{\sin(\alpha)^2 EI} \\ &\quad - \frac{1}{4} \frac{-2 R \sin(\alpha) - 2 R \alpha + 2 \sin(\alpha) R \cos(\alpha) + 2 R \cos(\alpha) \alpha}{R AE \sin(\alpha)^2} \\ F_{33}^0 &= \frac{\partial^2 U}{\partial n_i \partial n_i} = \frac{1}{4} \frac{R(-12 R^2 \sin(\alpha) + 12 R^2 \sin(\alpha) \cos(\alpha) - 4 R^2 \cos(\alpha)^2 \alpha - 4 R^2 \cos(\alpha) \alpha + 8 R^2 \alpha)}{\sin(\alpha)^2 EI} \\ &\quad - \frac{1}{4} \frac{-4 R^2 \sin(\alpha) + 4 R^2 \sin(\alpha) \cos(\alpha) + 4 R^2 \cos(\alpha) \alpha - 4 R^2 \alpha}{R AE \sin(\alpha)^2} \end{aligned} \quad (18)$$

### 3.4 Plastic rotation evolution laws

The element is completely defined introducing the yield functions of the plastic hinges  $i$  and  $j$ :  $f_i(\mathbf{M}, \Phi_p) \leq 0$ ,  $f_j(\mathbf{M}, \Phi_p) \leq 0$ . Then, plastic deformation evolution laws may be obtained via the conventional normality rule:

$$\dot{\phi}_i^p = \dot{\lambda}_i \frac{\partial f_i}{\partial m_i} + \dot{\lambda}_j \frac{\partial f_j}{\partial m_i}; \quad \dot{\phi}_j^p = \dot{\lambda}_i \frac{\partial f_i}{\partial m_j} + \dot{\lambda}_j \frac{\partial f_j}{\partial m_j}; \quad \dot{\delta}^p = \dot{\lambda}_i \frac{\partial f_i}{\partial n_i} + \dot{\lambda}_j \frac{\partial f_j}{\partial n_i} \quad (19)$$

where  $\lambda_i$  and  $\lambda_j$  are the plastic multipliers of, respectively, plastic hinges  $i$  and  $j$ , that may be computed by the usual consistency condition:

$$\begin{cases} \dot{\lambda}_i = 0 & \text{if } f_i < 0 \\ f_i = 0 & \text{if } \dot{\lambda}_i > 0 \end{cases}; \quad \begin{cases} \dot{\lambda}_j = 0 & \text{if } f_j < 0 \\ f_j = 0 & \text{if } \dot{\lambda}_j > 0 \end{cases} \quad (20)$$

It should be possible to include any of the conventional expressions for yield functions in the circular beam element: linear or no linear, with kinematic and/or isotropic hardening; even considering time-dependent plasticity is also possible. Therefore, the formulation could be used to analyze structures of any material, reinforced concrete, steel, aluminum and so on.

#### 4 NUMERICAL EXAMPLE

The arch element is thus defined by the kinematic equation and equilibrium (4), the elasticity law (16) and the plasticity laws (19-20).

The numerical implementation of the frame element does not require any special procedure. Any algorithm for the numerical analysis of elastic-plastic models with multiple yield functions can be used. For the example presented in this paper, an element compatible with a commercial structural analysis program [4] and an academic one [5] was developed and implemented. The program included the following yield functions:

$$f_i = |m_i - C\phi_i^p| - M_y; \quad f_j = |m_j - C\phi_j^p| - M_y \quad (21)$$

where  $M_y$  is the yield moment of the cross section and  $C$  is a plastic hardening/softening coefficient.

Figure 7 shows the geometry and the properties of a circular arch of radius 20 m. The structure was modeled using four elements with the same angle  $\alpha$  without taking the advantage of the symmetry. A displacement-controlled loading was applied in the middle of the arch and incremented monotonically up to the formation of plastic hinges on all the nodes.

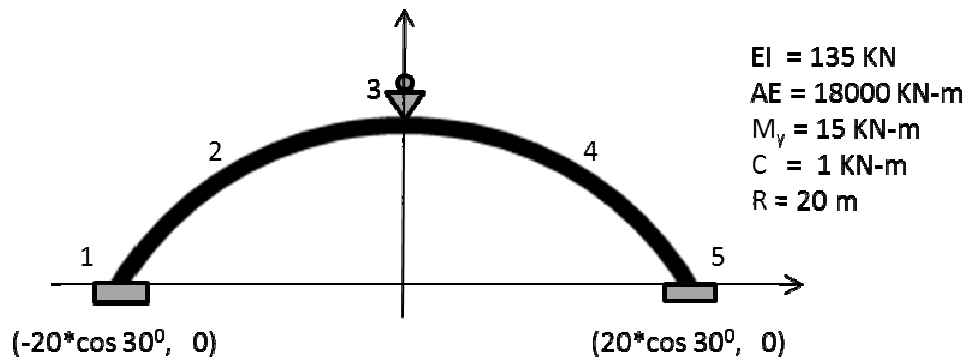


Figure 7. Geometry and properties of the arch

The curve of reaction force vs. displacement of the support in the middle of the arch is shown in Fig. 8. The bending moment diagrams at the times of the formation of plastic hinges are shown in Fig. 9, Fig. 10 and Fig. 11. In those figures, the bending moment is plotted against the angle  $\beta$  of each cross section. Fig. 9 corresponds to the time of formation of the first plastic hinge on the node 3; bending moments after the appearance of plastic hinges in 1 and 5 are shown in Fig 9. Fig 10 shows the distribution at the time of formation of the last plastic hinge. The corresponding deformed configurations of the arch are also included in the same figures. The final configuration of the arch is indicated in Fig 11.

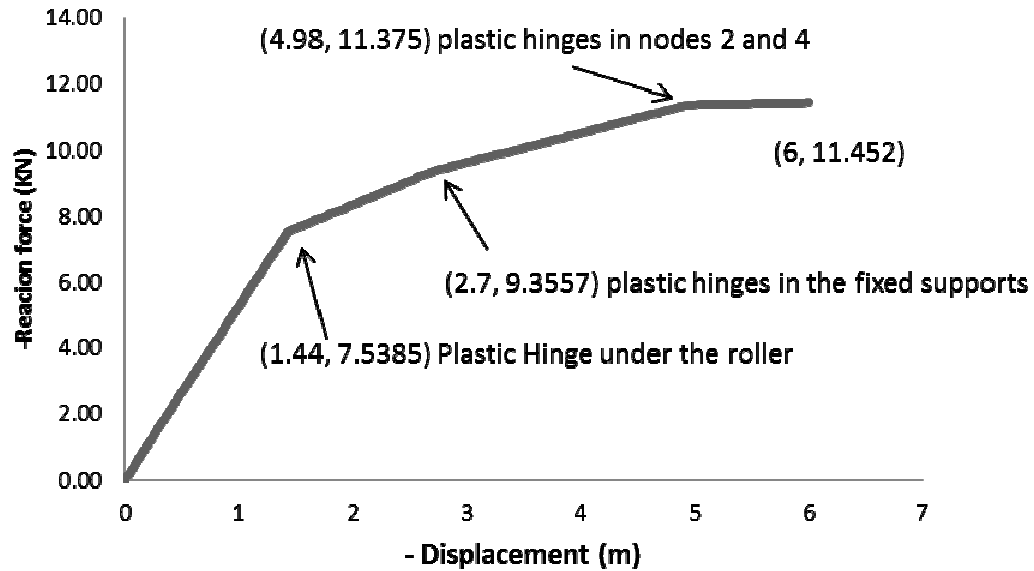


Figure 8. Displacement vs. force on the roller

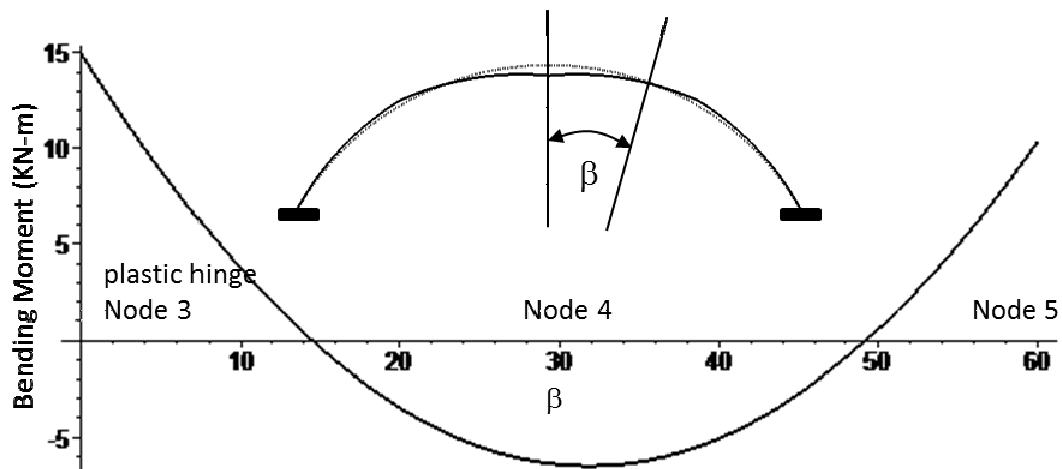


Figure 9. Distribution of bending moments on the arch after the appearance of the first plastic hinge

A similar, although not identical, structure was solved using a commercial finite element program: ANSYS [6]. The arch was discretized using three-node elements labeled in that program as BEAM 189. The same geometry was used in both cases but the ANSYS element includes plastic effects based on a fiber beam model; the uniaxial behavior of the material was represented using a yield function with linear kinematic hardening, yield stress of  $2222.22 \text{ KN/m}^2$  and a hardening coefficient of  $444.4 \text{ KN/m}^2$ . Fifty BEAM 189 elements of the same size were needed to reach a convergent solution that represents correctly the plastic zones. Fig 13 compares the proposed approach with the ANSYS solution using the displacement vs. force curve.

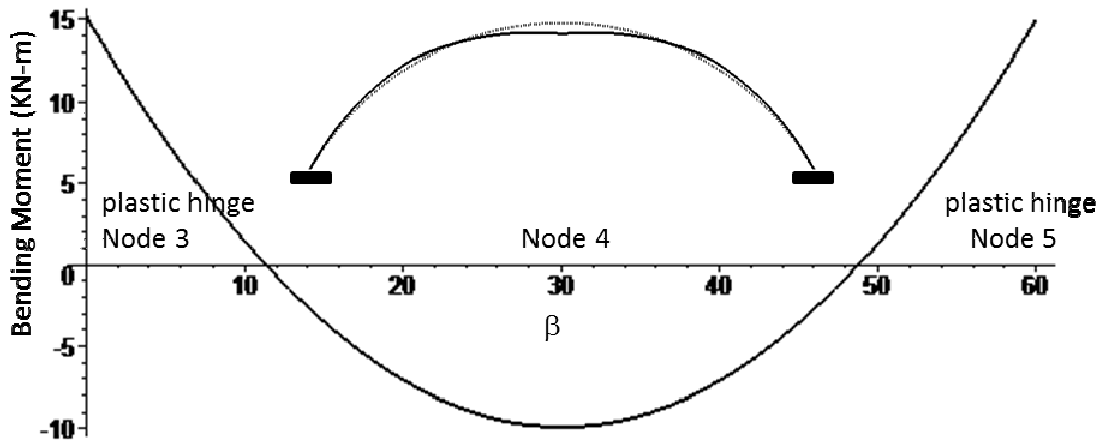


Figure 10. Bending moment distribution after the appearance of plastic hinges on the supports

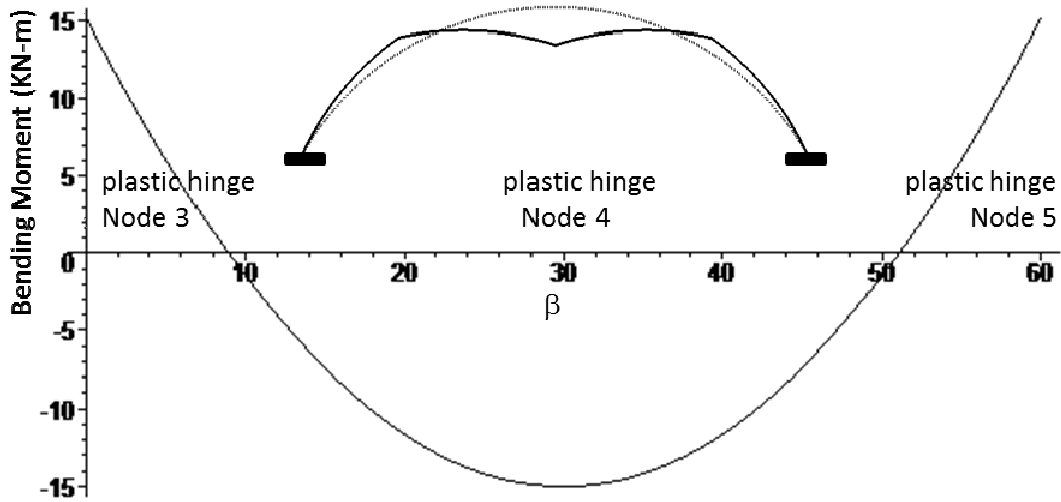


Figure 11 Bending moment distribution with plastic hinges on all the nodes

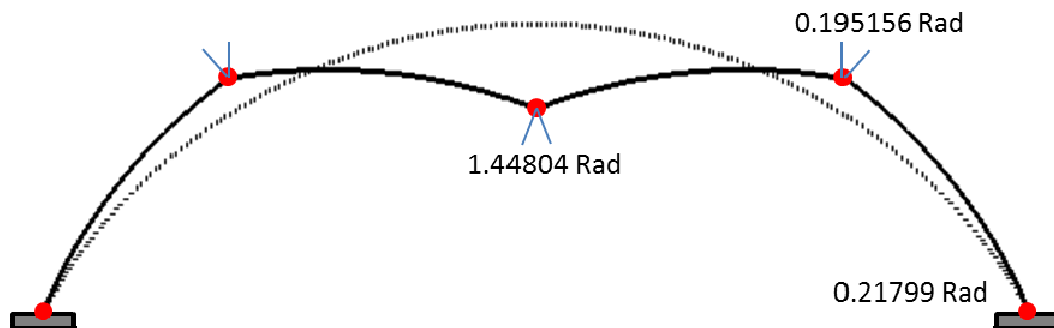


Figure 12 Initial and final configuration of the arch

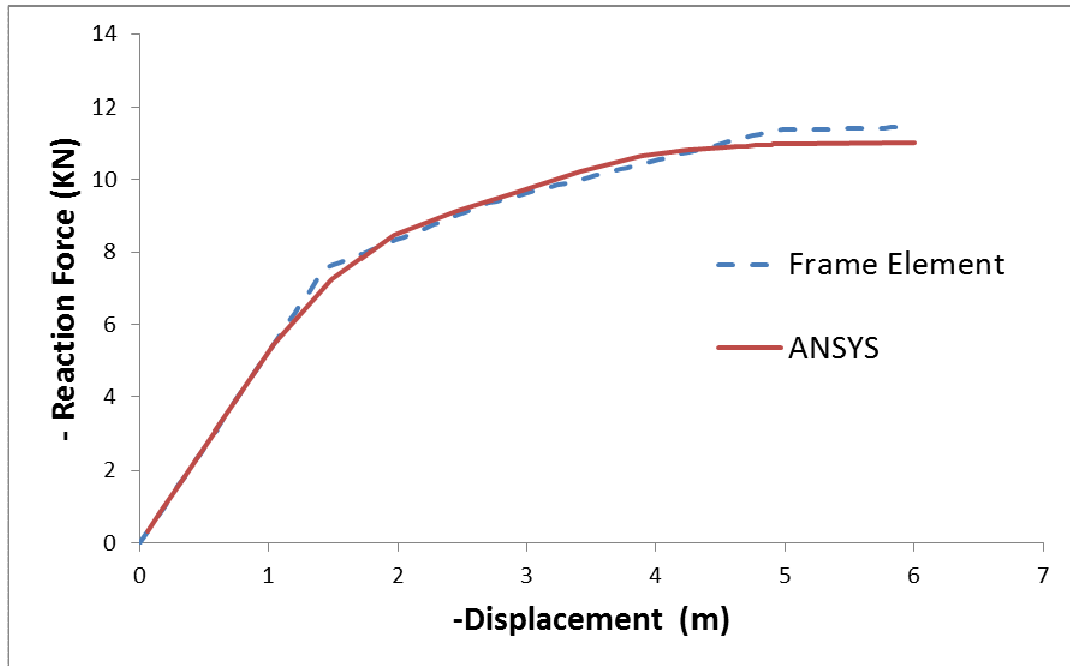


Figure 13 Comparison between ANSYS and the proposed analysis

## 5 CONCLUSION

The mathematical formulation of the element is very simple. Thus, not only numerical analysis, but analytical solutions as well can be obtained in many cases with the help of any symbolic manipulator program. This is not the case of the conventional beam elements.

Beyond the academic example included in the paper, it is clear that much more complex and realistic mathematical models describing the inelastic behavior of the hinges can easily be included in the element.

The consideration of some non-linear geometrical effects is also straightforward. It is sufficient to modify the linear kinematic and equilibrium equations used in the example by the non-linear versions also derived in the paper.

The behavior of a tridimensional frame element may be described by exactly the same matrix equations, expanding the matrices involved and reformulating the transformation and flexibility terms.

## ACKNOWLEDGEMENTS

The first author wishes to acknowledge the grant # 2012/02370-7 by FAPESP (FUNDAÇÃO DE AMPARO À PESQUISA DO ESTADO DE SÃO PAULO), Brazil.

## REFERENCES

- [1] R. Palaninathan and P. S. Chandrasekharan, (1985) "Curved beam element stiffness matrix formulation". *Comput. Struct.* 21, 663-669.

- [2] J.P. Marquist and T.M. Wang, (1989) “Stiffness matrix of parabolic beam element”. Comput. Struct. 31, 863-870.
- [3] H.G. Powell, (1969) “Theory for nonlinear elastic structures”. J. Struct. Div. ASCE (ST12) 2687-2701.
- [4] <http://www.3ds.com/products/simulia/portfolio/abaqus/overview/>
- [5] M. Uzcategui (2012) Implementation of finite elements in a web-based structural analysis program, thesis (in Spanish), University of Los Andes
- [6] <http://www.ansys.com/>